New Role of CFD in the Helicopter Design Process - The EC145 T2 Experience

Alessandro D'Alascio alessandro.dalascio@eurocopter.com

Klaus Kicker klaus.kicker@eurocopter.com

Thomas Kneisch thomas.kneisch@eurocopter.com

Stefanie Link stefanie.link@eurocopter.com

Tobias Ries tobias.ries@eurocopter.com

Dieter Schimke dieter.schimke@eurocopter.com

Aerodynamics Department
EUROCOPTER, Donauwörth, Germany

The EC145 T2 is a new 3-4 ton class, twin-engine, multi-purpose helicopter. The first challenging industrial applications of a comprehensive CFD based complete helicopter methodology were made to improve the handling quality of this machine in low speed flight conditions, specifically in transition flight from hover to forward flight and in quartering or lateral flight conditions. In these flight conditions the helicopter speed is of the same order of magnitude of the main and Fenestron® rotor induced velocities, so that none of the above mentioned air-flows dominates. Advanced coupled methods based on Computational Fluid Dynamics, inherently able to model aerodynamic interaction phenomena once sufficient wake conservation and a certain degree of modelling accuracy is assured, helped first to understand these complex aerodynamic interaction phenomena and then suggested solutions to improve the aerodynamic characteristics, in our case, of the tail unit. The effect of these solutions could be numerically verified via new computations before testing them in development flight campaigns. The paper shows two application examples of this CFD based methodology, which lead to an improved tail unit of the new EC145 T2 helicopter.

1 INTRODUCTION

During the last decade Computational Fluid Dynamics experienced an important progress, which widened the spectrum of applications in industry, now covering the whole development process of the helicopter ranging from early development to certification. Some applications, such as aerodynamic surface optimisation, computations of aerodynamic surface loads, polar generations, are well established; while others like free flight trimmed simulations about a complete H/C are being recently validated and run [1].

Indeed, in the early development phase of a new H/C or of an upgrade of an existing one, as soon as a CATIA model of the new or modified machine is available, together with a first version of its aeromechanic model, trimmed complete H/C simulations are viable by means of coupled CFD-CSM solvers. These powerful but CPU-time consuming methods can be applied to simulate flight conditions, in which strong aerodynamic interaction phenomena between rotors and fuselage occur, to fine tune the same aeromechanic models, which are then used intensively to analyse the H/C handling qualities.

At a later stage the same coupled CFD-CSM methods can support the aerodynamicist to analyse in detail interactional phenomena and suggest solutions to improve the flight-mechanic properties of an H/C during the first development flights tests.

The paper presents applications of this new CFD-CSM coupled methodology to achieve the aerodynamic design freeze of the empennage of the EC145-T2 helicopter. Two flight conditions are analysed in detail, low speed conversion flight and lateral flight.

2 ACRONYMS AND SYMBOLS

ADT	Alternating Digital Tree
ALE	Arbitrary Lagrangian Eulerian
CFD	Computational Fluid Dynamics
CG	Centre of Gravity
Cp	Pressure coefficient = $½\rho v^2$
CPU	Central Processing Unit
CSM	Computational Structural Mechanics
FADEC	Full Authority Digital Engine Control
GCL	Geometric Conservation Law
H/C	Helicopter
JST	Jameson-Schmidt-Turkel
My	H/C pitching moment
OEI	One Engine Inoperative
RPM	Revolution per Minute

3 THE EC145-T2 HELICOPTER

The EC145-T2 is a new 3-4 ton class, twin-engine, multi-purpose helicopter accommodating up to 12 seats for pilot/s and passengers. It combines Eurocopter latest technologies with the proven design elements of the BK117 family. The helicopter is equipped with an advanced cockpit design, modern state of the art avionics, a Fenestron® anti-torque system and Turbomeca Arriel 2E engines with dual channel FADEC. The new designed Fenestron® in combination with improved main gearbox torque ratings and powerful engines results in significantly increased Hover and OEI performances especially in high altitudes.

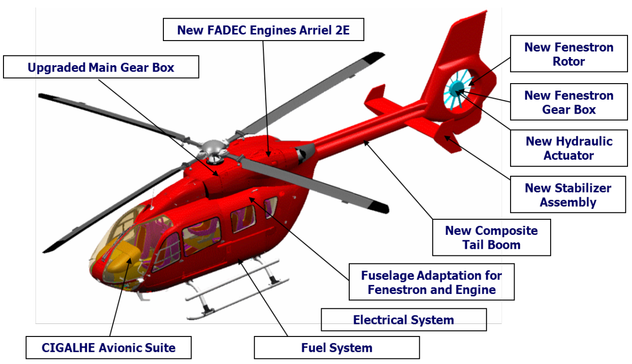

Figure 1: Novelties by the EC145-T2 Helicopter

4 COMPUTATIONAL METHOD

The chapter describes the numerical method used to perform free-flight trimmed complete H/C simulations as well as briefly the loose or periodic coupling methodology between CFD and CSM codes.

4.1 The CFD flow solver FLOWer

The CFD solver FLOWer [2] was developed by DLR in the framework of the MEGAFLOW project [4] and is available at Eurocopter through the cooperation with DLR in the framework of the research projects CHANCE [5], SHANEL [6] and MUSIHC.

FLOWer solves the three-dimensional, compressible and unsteady Reynolds-Averaged Navier-Stokes equations. The equations are formulated in a non-inertial rotating reference system with explicit contributions of centrifugal and Coriolis forces to the momentum and energy equations. Furthermore FLOWer includes the ALE-Formulation which facilitates the computation of deforming meshes by adding whirl-fluxes resulting from the cell face motion to the convective flux portion. The Geometric Conservation Law (GCL) evaluates the cell volumes of the deformable mesh consistent to the cell face velocities. This ensures the preservation of uniform flow on deformable grids.

The discretization of space and time is separated by the method of lines. FLOWer includes a cell-vertex and a cell-centred formulation. Convective fluxes are computed using the JST scheme [7] which uses 2nd order central differences with artificial dissipation for stabilization. The integration in pseudo time is carried out using a 5-stage hybrid Runge-Kutta method. In order to circumvent the time step limitation of the explicit scheme FLOWer makes use of the dual time stepping technique with a second order implicit time integration operator in case of unsteady flow [8].

FLOWer features the Chimera-technique allowing for arbitrary relative motion of aerodynamic bodies [3]. Relative motion of grids can be arbitrarily defined via the input file by setting up the required kinematic chain of coordinate systems. Chimera connectivity is determined using hole cutting and interpolation. The ADT search method is applied in order to identify donor cells in curvilinear grids.

Within the past years important additional helicopter specific features have been integrated into FLOWer by the Institute of Aerodynamics and Gasdynamics (University of Stuttgart) [9] and by Eurocopter. The so-called HELI version of the code includes interfaces for time-accurate and loose coupling, a multi-block blade grid deformation tool and rotor specific post-processing. Latest evolution of the code allows for fluid-structure coupling on multiple rotors and the modelling of deformable blade necks. The latter enables the simulation of elastically coupled rotor blades directly attached to a rotor head.

4.2 The CSM code CAMRAD II

The commercial aeroelastic analysis code for helicopters and rotorcraft CAMRAD II incorporates a combination of state-of-the-art technologies like multibody dynamics, nonlinear finite elements, structural dynamics and rotorcraft aerodynamics [10].

The aerodynamic modelling of rotor systems in CAMRAD II is based on lifting line theory assuming that the rotor blade has a high aspect ratio, or more generally that spanwise variations of the aerodynamic environment are small. This assumption allows splitting blade wing and rotor wake into separate models, which are solved individually and combined. Two-dimensional, steady airfoil data are extracted from airfoil tables for solving a two-dimensional wing aerodynamics. Code-internally, the coefficients are corrected for Mach and Reynolds effects, yawed flow and unsteady behaviour (Dynamic Stall modelling). With regard to wake modelling the induced velocity distribution on the rotor disk is either derived by analytical downwash models or computed by prescribed or Free-Wake methods.

CAMRAD II implements multibody dynamics to all structural elements subjected to rigid body motion with univocally defined kinematics of their interfaces. For the finite beam elements [11], the elastic motion is represented in addition by the deflection, elongation, and torsion of the beam axis. The beam element implemented in CAMRAD II offers three different geometric models ranging from exact kinematics of the beam elastic motion to retaining only second-order effects of elastic motion in the strain energy and kinetic energy, restricting the elastic motion to moderate deflection. The beam element features in addition two structural models. The first structural model is based on the beam theory for anisotropic or composite materials; the second structural model is based on Euler-Bernoulli beam theory for isotropic materials with an elastic axis, the undistorted elastic axis straight within the component. For the numerical model used in this paper, the second model was applied.

4.3 The loose or periodic coupling strategy

Loosely coupled simulations of isolated rotors are state-of-the-art at Eurocopter since several years. A loose coupling methodology [15], [16] between the CFD solver FLOWer and the comprehensive simulation codes HOST [9] and CAMRAD II [12] has been developed for this purpose. The tool chain has found its way into the industrial rotor design process. At the Institute of Aerodynamics and Gasdynamics (University of Stuttgart) the loose coupling methodology between FLOWer and HOST has been extended towards complete helicopter coupling [14].

For more details about the CFD-CSM coupling strategy and procedure refer to [1].

5 INVESTIGATED H/C GEOMETRIES

5.1 Baseline configuration

The baseline configuration, which has been aerodynamically investigated, is depicted in Figure 2. It features the EC145 cabin with a new Fenestron®, vertical fin, bumper and a horizontal stabiliser derived from the EC135. A simplified surface model of this geometry is depicted in Figure 3. It can be noticed that the landing skids have been omitted; the rotor head has been simplified by truncating its mast shortly before the engine cowling and omitting the pitch links rods, the scissors and the swash plate. The hole in the cowling through which the mast is connected to the main gearbox is closed and a gap between the mast and the cowling itself is assured. Moreover the ten stator blades in the Fenestron® duct are not modelled. All these simplifications were necessary to keep the meshing effort to a reasonable level and to save subsequently computational time. The decision not to account for the landing skids in the surface model of the baseline configuration was taken assuming that this component would not contribute to the phenomena, subject of study within the paper.

Figure 2: EC145-T2 baseline configuration (© Eurocopter)

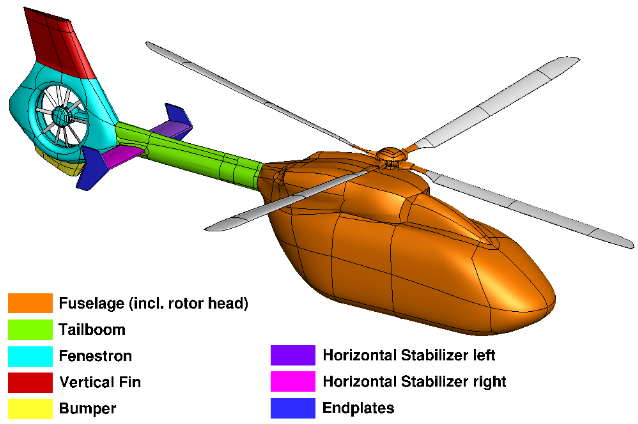

Figure 3: Surface model of the EC145-T2 baseline geometry subdivided in components

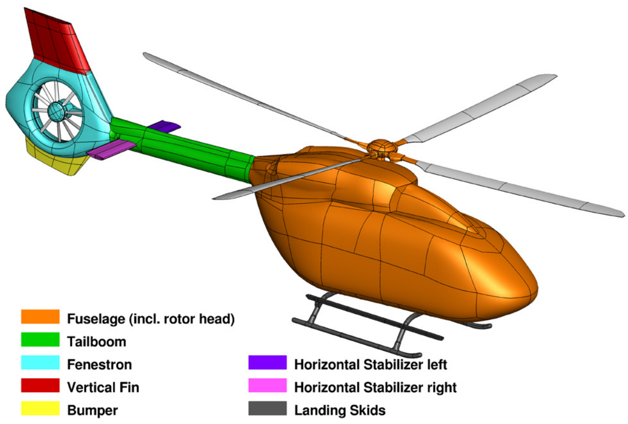

Figure 5: Surface model of the EC145-T2 improved geometry subdivided in components

5.2 Improved configuration

The differences between the improved configuration shown in Figure 4 and the baseline geometry concern the tail unit, i.e. the horizontal stabiliser has been taken from the BK117-C2 thus reducing its chord, the endplates have been dismounted, the vertical fin has been shortened, the bumper features a symmetric airfoil and a newly designed spoiler has been applied along the Fenestron® leading edge. The simplified surface model of the improved configuration (see Figure 5) features the same simplifications as the previous one but models the landing skids. Here it was decided to make an effort to implement the landing skids in the H/C model to verify numerically the previously mentioned assumption that the landing skids do not contribute to the phenomena object of this paper.

Figure 4: EC145-T2 improved configuration

6 MESHING STRATEGY

To model complete helicopter geometries, characterised by complex bodies in relative motion and subject to deformation, as slender rotor blades are, extensive use of overlapping body fitted and background meshes is made. The meshes about the baseline model were generated, first; subsequently, the grid system of the improved model was built starting from the previous one. For this reason the quality of the second mesh system is slightly higher than the one of the baseline model. To speed-up the mesh generation process, existing meshes were used as much as possible. The tail unit volume meshes, including the complete Fenestron®, were already available from previous isolated complete Fenestron® computations [1], as well as the fuselage [14] and the rotor head multi-block meshes. The blade meshes were also available. In fact, the work to set up the overlapping structured multi-block grid system was mainly invested in adapting and improving existing body fitted meshes, generating the intermediate and back-ground meshes and checking the chimera interpolations in the overlapping regions. Most of the engineer's work is thus spent in verifying that the overlap regions are large enough to allow for a correct Chimera tri-linear interpolation – this is done by fine tuning the dimensions and location of the masking meshes – and by assuring that overlapping cells are characterised by similar dimensions.

Figure 6 shows the hierarchical structure of both overlapping mesh systems. An automatically generated Cartesian background mesh contains the body fitted cabin and tail meshes. An intermediate Cartesian mesh, fully embedded in the background one, contains the blade and rotor-head meshes. The landing skids - when they are present - are embedded in the cabin mesh, whereas the tail mesh contains the duct and the Fenestron® rotor meshes: hub and blades. The rotating meshes are depicted in red in Figure 6. The horizontal stabiliser and endplates of the baseline configuration are part of the tail unit multi-block mesh, whereas they are modelled via chimera overlapping technique in the improved configuration. This was done to allow for an easy pitch attitude adjustment whenever necessary.

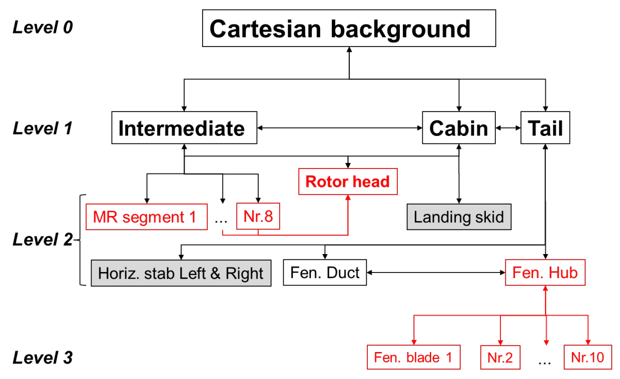

Figure 6: Hierarchical structure of the overlapping mesh systems

Figure 7 depicts the tail and cabin (level 1) and the blade horizontal stabiliser and landing skid (level 2) multi-block meshes around the surface geometry of the same configuration.

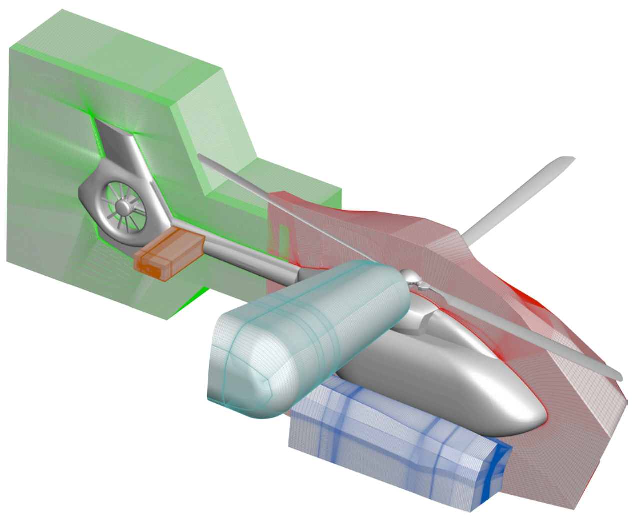

Figure 7: Chimera volume mesh system about the EC145-T2 improved geometry

The mesh system characteristics in terms of number of blocks and number of cells for each multi-block grid of the chimera mesh system are listed in Table 1. Globally the mesh system of the improved configuration is composed of about 64 million cells distributed over 1736 blocks, whereas the mesh system of the baseline configuration is composed of about 49 Million cells, as it can be verified in [1].

Table 1: Data of the Chimera mesh system about the improved model of the EC145-T2 H/C

Mesh component	Blocks	Cells
Background	72	1845248
Intermediate	108	9332480
Cabin	186	4089146
Tail	449	8509056
Main rotor blade	4 x 25	4 x 1575424
Main rotor head	42	2048000
Main rotor blade necks	4 x 6	4 x 702464
Fenestron ® duct	106	6841344
Fenestron ® hub	179	6537216
Fenestron ® blade	10 x 5	10 x 580096
Horizontal stabiliser	2x 19	2 x 1006592
Landing Skids (LS)	2 x 181	2 x 3398144
Frw. junction LS-cabin	10	456192
Aft junction LS-cabin	10	432640
Total	**1736**	**63813376**

7 PITCH-UP SIMULATION RESULTS

7.1 The pitch-up phenomenon

Since flight conditions of a helicopter vary in a broad range, the air flow velocity induced by the main rotor, i.e. the rotor downwash, affects the tail unit and particularly the horizontal stabilising surfaces in various ways. The horizontal stabilizer is responsible for part of the fuselage steady download in hover and is marginally affected by the main rotor downwash in high speed conditions. Yet in transition between these two flight conditions the tail unit experiences a great change in the induced flow field, meaning the forces and efficiency of its lifting surfaces will change considerably. This change in aerodynamic forces acting on the tail unit leads either to a change in the helicopter fuselage pitch attitude, when the H/C features an articulated main rotor, or to a sensible increase in the rotor mast moments, if the H/C features a bearing-less or hinge-less main rotor. This phenomenon is typically called "hump phenomenon" or "pitch-up". For the EC145 T2 helicopter using a hinge-less main rotor the pitch-up phenomenon is reflected in a mast moment increase, which needs to stay below a given threshold.

7.2 Flight Test Conditions

The investigation of the pitch-up phenomenon for an EC145 T2 prototype machine was carried out about the baseline configuration at a flight speed of 30kt and about the improved configuration at three conversion speed values of 18kt, 26kt and 40kt. The flight tests were carried out without sideslip angle. In Table 2 an overview of the test conditions is provided.

Table 2: Flight test conditions

Configuration	Baseline	Improved
Flight speed	30kt	18/26/40kt
H/C weight	3730kg	3590kg
Pressure altitude	530m	153m
Outside air temperature	23°C	-3°C
Rotor RPM	387rpm	387rpm
Advance ratio	0.069	0.042-0.092

7.3 Analysis of results

As already mentioned, one difference between the CFD-CSM setup of the baseline and improved configuration is the fact that the landing skids were omitted in the first one. The decision based on the assumption that these landing skids have a marginal influence on the H/C pitch-up behaviour can be verified through a component breakdown of the pitching moment around the centre of gravity, as shown in Figure 8. The contribution of the landing skid is negligible for the improved configuration at all investigated speeds as it can be verified in Figure 9. As expected the removal of the endplates and the chord reduction of the horizontal stabilizer results in a decrease of the down force and therefore of the pitching moment. The higher counter-oriented moment of the fuselage for the baseline configuration can be explained by the higher weight, and therefore by the increased downwash on the front part of the fuselage. The vertical fin shows a minor contribution, especially for the improved configuration with the shortened fin.

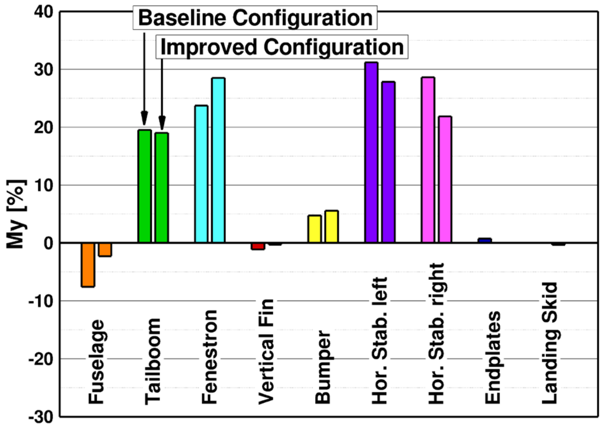

Figure 8: Pitching moment (CG) breakdown over the H/C components for the baseline and improved configurations respectively at 30kt and 26kt.

In Figure 9 the pitching moment break down versus flight speed of the improved configuration is illustrated. One can notice that the contribution to the pitching moment of the tailboom reduces by increasing the H/C forward speed, while the same contribution to the pitching moment of the horizontal stabilizer increases. This is due to the combination of the main rotor downwash with the H/C flight speed, thus to the resulting angle of the air flow impinging the tail unit and its velocity. Figure 10 depicts the stream-traces around the horizontal stabilizer and the effect of the H/C flight speed on the rotor wake direction. Clearly at 40kt the horizontal planes experience a higher air flow velocity at a smaller angle of attack thus generating higher down forces.

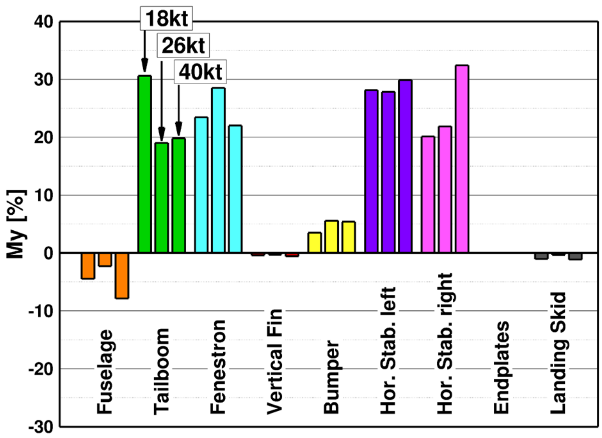

Figure 9: Pitching moment (CG) breakdown over the H/C components for the improved configuration at 18kt, 26kt and 40kt.

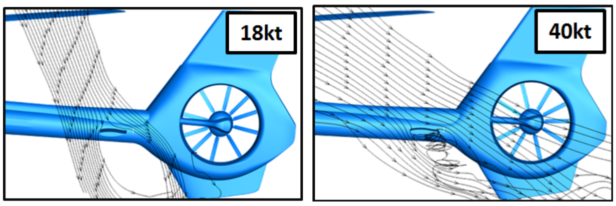

Figure 10: Stream-lines about the horizontal stabilizer of the improved configuration (circa 70% span-wise position)

As already mentioned, during the pitch-up phenomenon high hub pitching moments are generated. In Figure 11 the correlation of the hub pitching moment versus flight speed is shown. The expected distribution of pitching moment is based on Flight Test results with a similar configuration as the improved one. Relative Pitching Moments below 20kt and above 35kt, as well as a maximum nearby 26kt, are correctly reproduced by the CFD-CSM-coupled simulations of the improved configuration. One can also observe the reduction in pitching moment experienced by the improved configuration compared to the baseline, which clearly shows the effect of the configuration change.

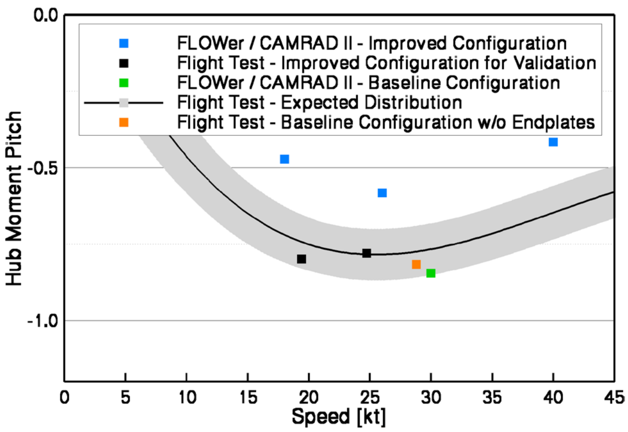

Figure 11: Hub pitching moment versus flight speed

A better compliance with flight test results would be desirable; but, considering that flight testing at such low speeds are more sensitive to wind conditions and aerodynamic interferences than corresponding ones at higher speeds and that the pilot is constantly obliged to adjust the H/C flight attitude, it is very difficult to find a good steady flight test point to be compared to a steady CFD-CSM-coupled simulation. Indeed the wind has a non-negligible effect on the air flow around the H/C and changes in the wind speed and direction manipulate the testing results. Moreover, during flight tests the H/C is subject to accelerations, therefore inertial moments sum-up to the aerodynamic ones. This is of course not the case for the steady CFD-CSM-coupled simulations and could partly explain the disagreement.

8 LATERAL-FLIGHT SIMULATION RESULTS

Strong interactions between the main rotor wake and other parts of the helicopter do not only occur in forward flight, like in the pitch up case, but also for other flight directions such as in sideward flight. In sideward flight especially the empennage and the anti-torque system can have a significant influence on the helicopters behaviour. Due to their big distance to the centre of gravity of the helicopter, already small changes in the forces on these parts can cause high changes in the moment equilibrium of the helicopter. Such force-changes can be caused by unsteady flow separations or by variations in the interactions between the main rotor downwash and the empennage or the anti-torque-system due to modifications in the H/C flight state. Therefore it is important to minimize the areas of unsteady separations and high force changes by slight changes of the flight attitude in sideward-flight. The most significant impact on the moment equilibrium in sideward flight can be expected in the yaw axis. Potential areas at which downwash interaction or separation could occur are all vertical surfaces, namely endplates, vertical fin, Fenestron®-shroud, bumper and tail-boom. During flight tests, some interaction phenomena or unsteady separations can easily be identified by removing single parts, but this is just possible for some parts like the bumper or the endplates. Flight tests showed that, for example, removing the endplates lead to a significant improvement in the yaw behaviour of the EC145-T2 in sideward flight conditions. However it is difficult to differ between interaction- and unsteady separation effects by the flight recording data and therefore the possibility to draw conclusions on the phenomena is limited. A CPU-time consuming complete helicopter CFD-CSM-coupled simulation is affordable just for few selected flight states, but it allows for a detailed analysis of unsteady separations at all individual H/C components and downwash-component interactions.

Table 3: Flight test conditions

Configuration	Baseline	Baseline with shroud-spoiler
Flight speed	35kt	35kt
Yaw Angle	300°	300°

To have a better insight in the aerodynamics in lateral flight conditions to the left of the EC145 T2 baseline configuration of paragraph 5.1, a complete helicopter simulation was carried out. It should be mentioned, that due to restrictions of computational power and time, the flight was not fully trimmed, but the attitude of the helicopter was set to realistic values provided by the flight test. The numerical analysis served to answer the question, first, why the removal of the endplates in the flight test improved the yaw behaviour in sideward flight and second to identify further potential sources for unsteady or interaction behaviour. For the analysis of the endplates, the flow-field was checked for a potential main rotor downwash interaction. At a given time instant a number of streamlines seeded in the vicinity of the endplates have been generated in the flow field upstream and downstream of these seeding points. The resulting stream lines are depicted in Figure 12.

It can be seen, that part of the streamlines can be followed to a tip vortex of the main rotor downwash and a part leads to the free-stream inflow. It can also be seen, that a separation zone forms on the right side of the endplates. From this it can be concluded, that the endplates are located at the edge of the interaction region of the main rotor downwash. Depending on the attitude of the helicopter, the inflow therefore can come either from the undisturbed free-stream or from the highly unsteady flow of the tip vortices with strong velocity gradients. Therefore, small changes in the attitude of the helicopter can lead to strongly changing velocities on the endplates and by that to significant moment variations in yaw.

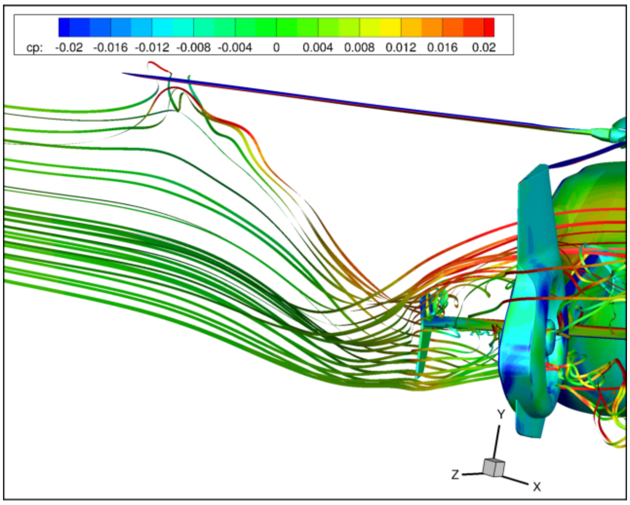

Figure 12: Sideward flight to the left. Streamlines showing main-rotor and free flow – endplate interaction

In order to identify further potential sources for unsteady interaction, the flow field was investigated with regard to three criteria. The *first* criterion was, to identify other areas of a strong main rotor downwash interaction, especially with regard to main rotor blade tip vortex interactions. *Second*, to identify regions of low pressure coefficients c_p which indicate high velocities and strong forces, and *third* to search for areas where small changes in the attitude of the helicopter might cause strong changes in the flow-field. Finally an area was identified which fulfilled all three criteria. On the right side of the leading edge of the Fenestron®, a field of very low pressure coefficients c_p was observed as depicted in Figure 13.

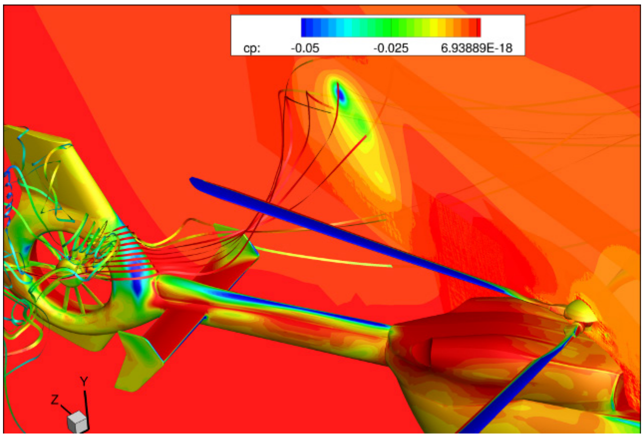

Figure 13: Sideward flight to the left. Streamlines showing main-rotor – endplates – Fenestron®-shroud interaction

In addition the majority of the streamlines starting at this area can be followed to the tip vortex of the main rotor downwash similar to the case for the endplates and is also depicted in Figure 13. It can also be seen by the streamlines downstream of the low pressure region that they continue into the Fenestron®. This indicates that the downwash is also interacting with the Fenestron® and that a slight change in the flight attitude, leading to a different Fenestron® shroud interaction, could also lead to different flow in the Fenestron® area, which increases the probability of force changes of the Fenestron®. Also due to the fact that the low pressure region is located on a round surface without any defined edge, which could trigger the flow separation, it is possible, that such flow separation changes position with changing the flight state. Therefore a geometry was required, which, on the one hand, could eliminate this potential source of unsteady behaviour in sideward flight to the left, and on the other, did not influence all other flight states. The solution for this problem is depicted in Figure 14. The spoiler A was mounted on the front side of the Fenestron® shroud in the area of the low pressure region. In sideward flight conditions to the left it triggers flow separation and inhibits reattachment downstream on the right surface of the Fenestron®-shroud. So the low pressure region at the side of the Fenestron® shroud is eliminated. In addition, the flow separation-line is fixed to the edge B, shown in Figure 14, for a wide range of yaw inflow conditions, so that unsteady forces caused by a moving separation-line are inhibited. To avoid deteriorating the H/C flight behaviour in any other flight condition, the spoiler geometry was closed and smoothly blended with the shroud on side C, to avoid flow separations in forward flight and sideward flight to the right, for example.

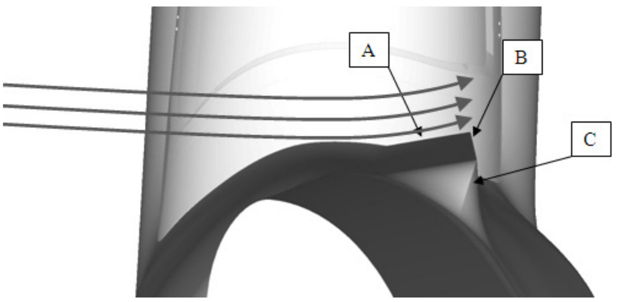

Figure 14: Spoiler at Fenestron® shroud for flow redirection and a defined separation point.

After the geometric definition of the spoiler, the configuration was again simulated in CFD and it could be shown, that the flow was changed as required. Flight tests were carried out in order to investigate the functionality of the spoiler. It was proven that the spoiler significantly improved the yaw stability in lateral flight and did not deteriorate the behaviour in any other flight condition either.

The spoiler effect on the yaw moment generated by the Fenestron®-shroud (left and right side) is depicted in Figure 16. Here it can be observed how applying a longitudinal spoiler along the shroud leading edge the yaw moments oscillations could be sensibly reduced, thus improving the H/C handling quality in lateral flight.

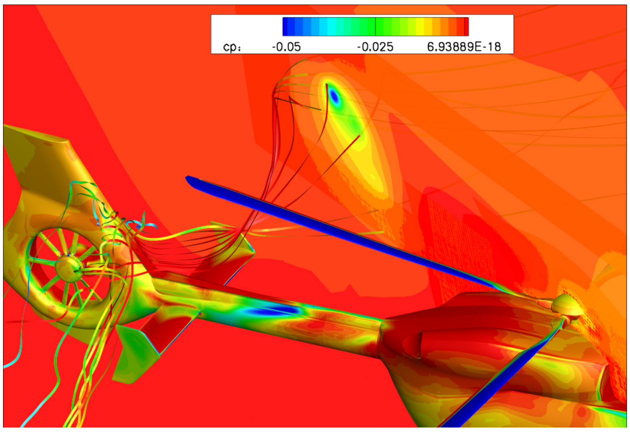

Figure 15: Sideward flight to the left. Streamlines showing main-rotor – endplates – Fenestron®-shroud interaction with spoiler

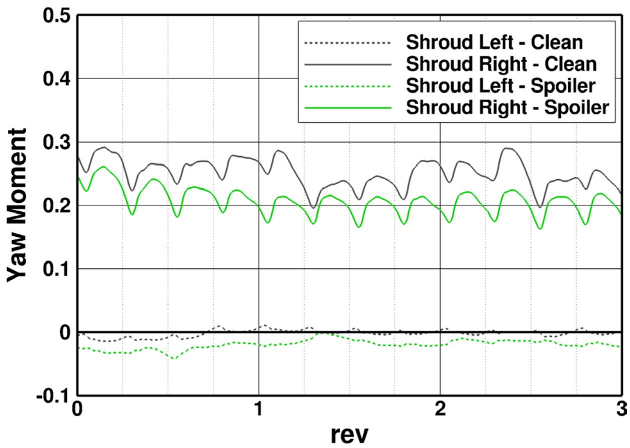

Figure 16: Comparison of Yaw Moment (CG) behaviour on the left and right side of the Fenestron® box

9 CONCLUSIONS AND OUTLOOK

In the paper the application of CFD-CSM-coupled complete helicopter simulations, which assisted the aerodynamic design freeze of the EC145 T2 empennage is presented. Therefore two different helicopter configurations have been investigated, a baseline and an improved version. Major changes of the improved configuration were a chord reduction of the horizontal stabilizer, the removal of the endplates and a newly designed spoiler located along the leading edge of the Fenestron®.

Flight conditions characterised by strong aerodynamic interactions were examined:

1. EC145 T2 numerical investigations in conversion from hover to forward flight, with flight speeds ranging from 18kt to 40kt, revealed a negligible influence of the landing skids on the hub pitching moment, whereas tailboom, Fenestron® and horizontal stabilizer were identified as main the contributors. A reduction of pitching moment was shown from the baseline to the improved configuration. This reduction was achieved by reducing the horizontal stabiliser chord and dismounting its endplates.

2. Lateral flights to the left have been simulated in order to identify the reasons and sources of unsteady yaw behaviour. Numerical simulations highlighted interactions between the main rotor tip vortices and parts of the empennage and the Fenestron® shroud. The beneficial effects of removing the endplates during flight tests could be explained by the simulations. Moreover, a deeper analysis of the simulation results gave the aerodynamicists the idea to design a spoiler to be placed along the leading edge of the Fenestron®-shroud which would reduce the yaw moment generated by the shroud right surfaces. Finally the effectiveness of the spoiler was proven in flight and retained for the improved configuration.

These two examples show how CFD-CSM coupled complete helicopter simulations can reduce the number of required flight testing hours to reach aerodynamic design freeze and to bring a clearer understanding of specifically flight condition dependant phenomena. Moreover, a deeper insight in interactional aerodynamic phenomena, gained by applying such computational intensive methods, paves the way to analytical or numerical improvements of low fidelity but faster methods. Finally trimmed complete H/C simulations by means of coupled CFD-CSM solvers can be used in the, H/C product development cycle from feasibility and pre-design, through detailed design, till support to flight testing whenever a deeper understanding of the local and global aerodynamic phenomena of the complete helicopter is required.

10 ACKNOWLEDGEMENTS

The authors would like to thank the German ministry of Economy and Labour (BMWA) for its funding in the framework of ECO-HC 2 (grant 20H1103).

11 REFERENCES

[1] Dietz, M., Kneisch, T., Roth, G., D’Alascio, A., Schimke, D.: EC145 T2: Comprehensive and challenging industrial CFD applications. American Helicopter Society 68th Annual Forum, Fort Worth, Texas 1-3 May, 2012.

[2] Kroll, N., Eisfeld, B., and Bleecke, H.M. “The Navier-Stokes Code FLOWer”, volume 71 of Notes on Numerical Fluid Mechanics, pages 58-71. Vieweg, Braunschweig, 1999.

[3] Schwarz, T.: The Overlapping Grid Technique For The Time Accurate Simulation of Rotorcraft Flows. Proceedings of the 31st European Rotorcraft Forum, September 2005

[4] Kroll, N.; Rossow, C.-C.; Becker, K.; Thiele, F.: The MEGAFLOW Project. In: Aerospace Science and Technology, Vol. 4, 2002, pp. 223-237

[5] Costes, M., Pahlke, K., D'Alascio, A., Castellin, C., Altmikus, A.: “Overview of results obtained during the 6-year French-German CHANCE project”, AHS 61st Annual Forum, Grapevine, TX, June 2005.

[6] Costes, M., Raddatz, J., Borie, S., D’Alascio, A., Embacher, M.: “Advanced Rotorcraft Aeromechanics Studies in the French-German SHANEL Project”, Proceedings of the 35th

European Rotorcraft Forum, Hamburg, Germany, September 2009.

[7] Jameson, A., Schmidt, W., Turkel, E.: “Numerical Solutions of the Euler Equations by Finite Volume Methods Using Runge-Kutta Time-Stepping Schemes”, AIAA-Paper 81-1259, 1981.

[8] Jameson, A.: “Time Dependent Calculation Using Multigrid, With Applications to Unsteady Flows Past Airfoils and Wings”, AIAA-Paper 91-1596, 1991.

[9] Dietz, M.: „Simulation der Umströmung von Hubschrauberkonfigurationen unter Berücksichtigung von Strömungs-Struktur-Kopplung und Trimmung“, PhD Thesis, Verlag Dr. Hut, ISBN 978-3-89963-942-1, 2009.

[10] Johnson, W.: “Technology Drivers in the Development of CAMRAD II”, AHS Aeromechanics Specialists’ Conference, San Francicso, CA, 1994.

[11] Johnson, W.: “Rotorcraft Dynamics Models for a Comprehensive Analysis”, AHS 54th Annual Forum, Washington, DC, 1998.

[12] Dietz, M., Dieterich, O.: Towards Increased Industrial Application of Rotor Aeroelastic CFD. Proceedings of the 35th European Rotorcraft Forum, Hamburg, Germany, September 22-25, 2009.

[13] Dietz, M., Maucher, Ch., Schimke, D.: Addressing Today’s Aeromechanic Questions by Industrial Answers. Proceedings of the American Helicopter Society Aeromechanics Specialists’ Conference, San Francisco, CA, January 20-22, 2010.

[14] Embacher, M., Keßler, M., Dietz, M., Krämer, E.: Coupled CFD-Simulation of a Helicopter in Free Flight Trim. Proceedings of the American Helicopter Society 66th Annual Forum, Phoenix, AZ, May 11 – 13, 2010.

[15] Servera, G., Beaumier, P., Costes, M.: “A weak coupling method between the dynamics code HOST and the 3D unsteady Euler code WAVES”, Proceedings of the 26th European Rotorcraft Forum, The Hague, The Netherlands, September 2000.

[16] Potsdam, M., Yeo, H., Johnson, W.: “Rotor Airloads Prediction Using Loose Aerodynamic/Structural Coupling”, AHS 60th Annual Forum, Baltimore, MD, June 2004.

12 COPYRIGHT STATEMENT